Salvador-Llàcer, P.; Valls Coquillat, J.; Corral, JL.; Almenar Terre, V.; Canet Subiela, MJ. (2022). Linear Response Modeling of High Luminous Flux Phosphor-Coated White LEDs for VLC. Journal of Lightwave Technology. 40(12):3761-3767. https://doi.org/10.1109/JLT.2022.3150907

Linear Response Modeling of High Luminous Flux Phosphor-Coated White LEDs for VLC

Pau Salvador, Javier Valls, Juan Luis Corral, *Senior Member, IEEE,* Vicenç Almenar, Maria Jose Canet

***Abstract*—The widespread deployment of LEDs for illumination purposes has open the door to the use of these devices for visible light communications (VLC). Most lighting fixtures are mounted with phosphor-based white LEDs, and a driver connected to the LED is also required for VLC. This paper shows that the parasitic effects introduced by this setup change the frequency response of the intrinsic LED. A linear model to characterize the whole setup is proposed, as well as a methodology to extract its parameters. This methodology allows the designer to characterize the frequency response of LEDs without the additional difficulty of knowing the specific parasitic components introduced by the setup. The proposed model offers an accurate estimation of the slope of the LED frequency response in order to broaden the frequency range in which the model is useful to characterize and simulate VLC links. This was corroborated with the characterization of three commercial white LEDs whose measured and modeled frequency responses matched perfectly.**

***Index Terms*—White LED, linear model, VLC.**

I. Introduction

VISIBLE Light Communications (VLC) are gaining a lot of research interest in recent years as a wireless communication technology for indoor environments, thanks to the increasing use of LEDs for lighting [1], [2]. In VLC, LED lamps are not only used for lighting, but also for data transmission using intensity modulation.

White light LEDs are mostly based on two technologies: RGB LEDs or phosphor-coated blue LEDs. In the RGB case, three LEDs emitting red, green and blue lights must be driven with proper intensities in order to generate white light by color addition. In the phosphor-coated case, thanks to the fluorescence of the phosphor material, part of the blue light emitted by one blue LED is converted to yellow light with a broad spectral distribution when it goes through the phosphor coating. The combination of blue and yellow lights renders white light. Phosphor-based white LEDs are preferred for lighting due to their lower cost and their simpler driving circuits.

The classical small-signal model for an LED is based on a 1^{st}-order RC circuit [3]. However, the range of phosphor-based white LED models for VLC available in the literature is quite diverse. Some authors use an empirical 1^{st}-order function ($H(f)=e^{-f/f_P}$) with no physical explanation [4], [5], [6]. Other authors focus on the low pass effect of the phosphor coating, sometimes combined with the classical 1^{st}-order response of an LED [7], [8]. In [8] the LED frequency response is modeled as a linear combination of a 1^{st}-order response due to the blue light component (which only depends on the lifetime of the blue LED minority carriers) and a 2^{nd}-order response for the yellow light (which adds the dependence on the phosphor radiative lifetime to the blue LED response). These models have shown to work properly for some specific and controlled scenarios. However, different models are required in VLC LED lighting implementations or when the full LED bandwidth is used.

Recently, the impact of parasitic components on the frequency response of white LEDs has been highlighted [9], [10], [11], so that they have been included in the LED electrical model. For example, the measurements in [11] suggested that a 2^{nd}-order behavior in the frequency response is due to those components. On the other hand, although the circuit models proposed in [9] and [10] have orders higher than 2, their measurements and estimations show that the 2^{nd}-order behavior dominates at lower and medium frequencies and the higher poles appear at very high frequencies, i.e. around $400-500$ MHz. Additionally, it was already stated in [12] that commercially packaged white LEDs have significant series inductance. This inductance causes the 1^{st}-order LED model to become a 2^{nd}-order model. Even though the circuital models are appropriate for the characterization of this higher order behavior of the blue component of the LED, they fail to take into account the influence of the phosphor coating.

A real lighting scenario (e.g. an office building) requires high luminous flux LEDs. Those LEDs, in fact, are composed of several LEDs combined in serial or parallel within the same package. This package is welded to a heat sink socket, which in turn is welded to a support that acts as a radiator (to facilitate heat dissipation) and probably as a reflector of light. When data transmission is added to a lighting LED, a driver and a bias-T are needed to modulate the LED, and they are usually set on a printed board, which is placed behind the radiator and connected with wires to the LED socket. In this realistic setup *e.g.* the one shown in Fig. 1), the parasitic effects described in [9], [10], [11] will probably appear and affect the frequency response of the intrinsic LED.

In this paper, we analyze and model the behavior of high luminous phosphor-coated white LEDs; the contributions of this work are the following:

Grants RTI2018-101658-B100, RTI2018-101296-B-I00 funded by MCIN/AEI/10.13039/501100011033 and by "ERDF A way of making Europe", by the "European Union". and grant FPU19/04648 by Ministerio de Ciencia, Innovación y Universidades para la Formación de Profesorado Universitario.

P. Salvador, J. Valls, V. Almenar, and M.J. Canet are with the Instituto de Telecomunicaciones y Aplicaciones Multimedia, Universitat Politècnica de València, Valencia 46730, Spain (e-mail: pasallla@upv.es; jvalls@upv.es; valmenar@upv.es; macasu@upv.es).

J.L. Corral is with the Instituto Universitario de Tecnología Nanofotónica, Universitat Politècnica de València, Valencia 46730, Spain (e-mail:jlcorral@upv.es).

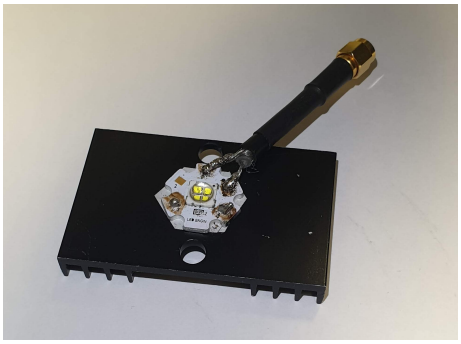

Fig. 1. VLC LED mounted on a lighting fixture

- A model for white LEDs that, like [7] and [8], separates blue diode and phosphor coating effects. In this paper a 2^{nd}-order transfer function is considered to characterize the blue diode, which is required to represent the behavior of the LED in a realistic lighting environment.
- A compact expression for the linear model of the white LED, which includes three poles and one zero. The poles are directly obtained from the frequency response of the blue and the yellow light components. The frequency of the zero is shown to depend on the power ratio of the detected blue and yellow lights and its influence in the white LED frequency response partially counterbalances the effect of the blue LED higher pole.
- A systematic method to extract the parameters of the model, which requires only three frequency response measurements. This method was validated using three high luminous flux white LEDs with different features.

The rest of the paper has the following structure: Section II, introduces the circuital model of the blue component of a white LED; Section III details the proposed linear model for the white LED; Section IV presents the method to extract the parameters of the model, the characterization of three LEDs using this model, and the analysis of results. Finally, the conclusions are stated in Section V.

II. Circuital Model of Blue LEDs in Light Fixtures

It is well known that the small-signal behavior of an LED is like that of a 1^{st}-order system, whose circuit model is a resistance (r_d) and a capacitance (C_d) in parallel. Therefore, its ideal frequency response (Eq. 1) is that of a single pole low-pass filter with cutoff frequency $f_{-3dB}=1/(2\pi r_d C_d)$.

$$H_{Intrinsic\_LED}(s) = \frac{1}{r_d C_d s + 1} \tag{1}$$

However, when a high luminous white LED is mounted on a lighting fixture, its frequency response changes. The order of the system is increased due to the reactive parasitic elements and, in addition, the poles of the system also depend on the output impedance of the driver used to modulate the LED.

As an example to show this physical mechanism, the LED model with parasitic components of [11] and the formulation of [9], [10] are used. The circuital scheme of Fig. 2 represents the output stage of the driver (a voltage source V_s with its output resistance R_g), the equivalent model of the intrinsic LED (its dynamic resistance r_d and its junction capacitance C_d) and the parasitic inductance L_s and resistance R_s due to the LED package and the lighting fixture. The output of this circuital scheme, V_{PD}, corresponds to the voltage at the photodetector output as the gain coefficient h includes the effect of the LED efficiency, the channel attenuation, the photodetector responsivity and the gain of the transimpedance amplifier.

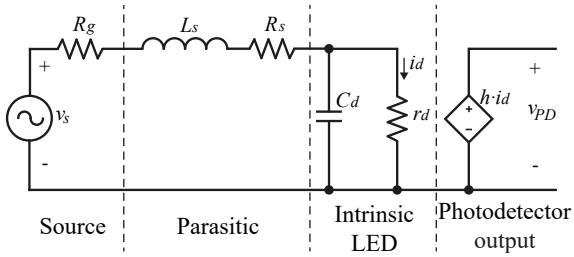

Fig. 2. Circuital model of an LED including the parasitic components and the driver output impedance.

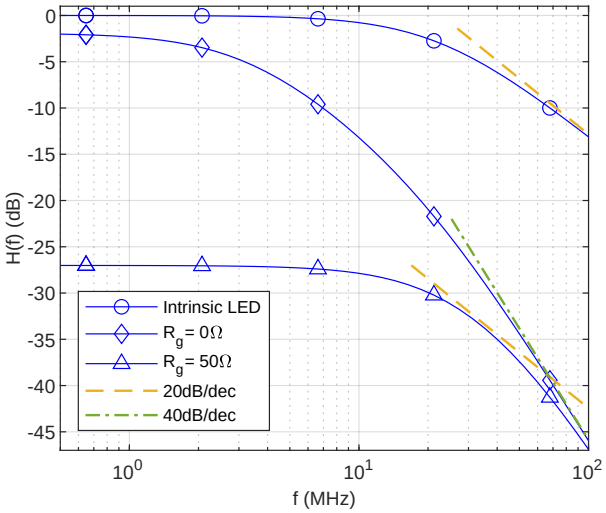

Fig. 3. Simulated frequency responses of $H_{Intrinsic\_LED}(s)$ and $\frac{V_{PD}(s)}{V_s(s)}$

The transfer function $\frac{V_{PD}(s)}{V_s(s)}$ is formulated in Eq. 2 and its poles in Eq. 3. Thus, the frequency response of the system depends not only on the intrinsic LED and parasitic components, but also on the output resistance of the driver, R_g. In any case, the frequency response corresponds to a 2^{nd}-order system due to the presence of the parasitic inductance and the capacitance of the intrinsic LED.

$$\frac{V_{PD}(s)}{V_s(s)} = \frac{h}{r_d C_d L_s s^2 + \left((R_g+R_s) r_d C_d + L_s\right) s + (R_g+R_s+r_d)} \tag{2}$$

$$s_{1,2} = -\left(\frac{R_g+R_s}{2L_s} + \frac{1}{2r_d C_d}\right) \pm \sqrt{\left(\frac{R_g+R_s}{2L_s} - \frac{1}{2r_d C_d}\right)^2 - \frac{1}{C_d L_s}} \tag{3}$$

In order to show an example of how the values of R_g and L_s impact on the frequency response, the values of the parasitic

components and the resistance and capacitance of our LED3 (detailed in Section IV) were estimated to match the blue LED frequency response (given in Fig. 9). Specifically, the intrinsic LED parameter values are r_d=2.36 Ω and C_d=2.98 nF; those of the parasitic components are R_s=0.58 Ω and L_s=165.6 nH. The frequency response of the ideal intrinsic LED and the response of the LED with parasitic components and driver with R_g=0 Ω are shown in Fig. 3. While the intrinsic LED has a single pole at 22.3 MHz, the system including the parasitics has two poles, one at 3.2 MHz and the other at 19.9 MHz. This causes a reduction in bandwidth and an increase in the response slope, approaching −40 dB/dec. As many researchers in their experiments drive the LEDs directly from signal generators or amplifiers, both with an output impedance of R_g=50 Ω, the frequency response of that case is also included in Fig. 3. This new scenario moves the poles to 24.8 MHz and 46.5 MHz and introduces a high attenuation due to the mismatch between the driver output impedance and the LED impedance.

Note that Eq. 3 gives real poles independently of the value of R_g in this example. This is due to the high value of the parasitic inductance caused by the lighting fixture and the connection to the driver (*i.e.* 330 nH were measured in [12] for a commercial LED). In fact, large values of L_s favor real poles in Eq. 3.

Based on results from previous authors and given the good agreement with our measurements, we make use of a 2^{nd}-order system with real poles to model the blue component of the LEDs in the next section.

III. Proposed LED model

The proposed model combines the effects from the blue LED and the phosphor coating, *i.e.* in a white LED made of a blue LED coated with phosphor, the white light is generated as the sum of two types of light: the one transmitted by the blue LED and the one emitted by the yellow phosphor. Therefore, both light sources can be modeled separately and subsequently added.

In the model definition, it is assumed that the optical power generated by the LED, $P_0(t)$, due to its modulating voltage, $v_s(t)$, is detected by a photodetector (PD) whose output voltage ($v_{PD}(t)$) is proportional to that optical power, as shown in Fig. 4(a). Therefore, although the white LED combines the electro-optical process of the blue LED with the fully optical process of the phosphor coating, the complete model can be written in the electrical domain. All DC or bias terms at the LED or PD are not considered in the model as we are only concerned with the data signals to be transmitted. The objective of this paper is to obtain a linear model of the relation between the photodetector output $V_{PD}(s)$ and the white LED input, $V_s(s)$, in the Laplace domain, $H_w(s)$.

The proposed linear model for the white LED shown in Fig. 4(b) is based on a linear combination of the detected blue and yellow light components, modeled as $H_b(s)$ and $H_y(s)$, respectively.

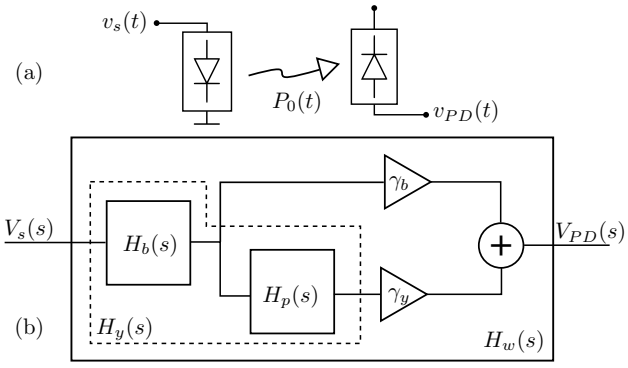

Fig. 4. (a) System to be modeled. (b) Block diagram of the complete model.

A. Linear model of blue LEDs

As stated in Section II the blue LED can be modeled as a 2^{nd}-order system with two real poles. Therefore, the transfer function of Eq. 3 can be rewritten like Eq. 4, whose real poles are $-p_{b1}$ and $-p_{b2}$, and k_b=$H_b(0)$.

$$H_b(s) = \frac{k_b}{(\frac{s}{p_{b1}} + 1)(\frac{s}{p_{b2}} + 1)} \tag{4}$$

B. Phosphor coating effect and yellow signal model

In a phosphor-based white LED, the layer of photoluminiscent material (typically YAG:Ce) absorbs most of the blue photons emitted by the blue LED and, after an excitation-relaxation process, new yellow photons at a longer wavelength are generated. The modulation bandwidth of the light coming from the white LED is reduced due to the time the YAG:Ce molecules stay in the excited state prior to the emission of the yellow photon. The average value of the relaxation process, this is, the fluorescence lifetime, is in the range of tens of ns for typical YAG:Ce materials [7]. After passing through the phosphor layer, the light emitted from the LED is a combination of blue and yellow photons, offering the desired white light. When this white LED is used for VLC data transmission, the fluorescence process adds a bandwidth limitation to the VLC link as the yellow emission process is not able to follow the fastest transitions of the incoming blue light.

The behavior of the phosphor coating is modeled like a 1^{st}-order system (Eq. 5), where $-p_p$ is a real pole and k_p=$H_p(0)$.

$$H_p(s) = \frac{k_p}{(\frac{s}{p_p} + 1)} \tag{5}$$

The model of the generated yellow wave is obtained as the cascade of the blue LED and the effect of the phosphor transfer functions, as in Eq. 6.

$$H_y(s) = H_b(s) \cdot H_p(s) \tag{6}$$

C. Complete model

In a phosphor-based white LED, the thickness and doping of the phosphor coating are selected to obtain the desired combination of blue and yellow lights so that the expected white light is rendered. The block diagram of the white LED complete model is detailed in Fig. 4(b) and formulated in Eq. 7, where γ_b and $\gamma_y \cdot k_p$ are the weights with which the blue and yellow components are added at the receiver, respectively. These weights take into account not only the relative proportion of both blue and yellow components in the white light, but also the different responsivities of the photodetector at each wavelength.

$$H_w(s) = \gamma_b \cdot H_b(s) + \gamma_y \cdot H_y(s) \tag{7}$$

This transfer function can be rewritten by substituting Eq. 4, Eq. 5 and Eq. 6 in Eq. 7, giving Eq. 8,

$$H_w(s) = \frac{k_T(\frac{s}{z_p}+1)}{(\frac{s}{p_{b1}}+1)(\frac{s}{p_{b2}}+1)(\frac{s}{p_p}+1)}, \tag{8}$$

where $k_T{=}k_b\gamma_b(1{+}\frac{k_p\gamma_y}{\gamma_b})$ and $z_p{=}p_p(1{+}\frac{k_p\gamma_y}{\gamma_b})$. Therefore, the complete model has one zero and three poles. The three poles in Eq. 8 correspond to the poles of the blue LED response, $H_b(s)$, and the pole of the phosphor response, $H_p(s)$. The frequency of the zero is slightly higher than the frequency of the pole coming from the phosphor coating. In fact, the position of the zero depends on the detected power ratio between yellow and blue lights, $k_p\gamma_y/\gamma_b$, in such a way that when there is more blue content the position of the zero is closer to the position of the pole coming from the phosphor response, $-p_p$ and partially compensates the effect of the pole in the frequency response. This effect will be experimentally shown in Fig. 10 in section IV.C.

On the other hand, our model allows us to derive some interesting conclusions, which are not easily extracted without Eq. 8. If the blue LED behaves like a 2^{nd}-order system, when the phosphor coating is added (which is a 1^{st}-order system), one could expect the complete white LED model to behave like a 3^{rd}-order system; however, that does not happen. This is due to the fact that the phosphor coating not only introduces a new pole in the yellow component frequency response, but also a new zero in the white light frequency response. This zero compensates the second pole of the blue LED in the white LED response at high frequencies. Note that if the blue LED could be modeled as a 1^{st}-order system, the same effect would appear: the phosphor would introduce a pole and a zero in the white light frequency response and the result for high frequencies would be a slope of -20dB/dec as if it were a 1^{st}-order system.

IV. White LEDs characterization

Fig. 5 shows the setup used in the model parameter estimation. The transmitter consists of an arbitrary wave generator (AWG) Siglent SDG6022X, an amplifier implemented with an OPA2677 (which has a low output impedance, lower than 1.8 Ω in the whole measurement range) and a bias-T with a capacity of 15 µF and an inductance of 1 mH, which are connected to the LED under test. At the receiver, the lens ACL25416U-A is used with the PDA10A amplified photodetector, which is placed at a distance of 75 cm and its output is connected to the Rohde&Schwarz RTM3004 oscilloscope (OSC). Both AWG and OSC are controlled from MATLAB to generate and capture the transmitted and received signal, respectively. Since the proposed method requires the independent measurement of white, blue and yellow components of the transmitted light, a blue filter (FGB25 from Thorlabs) or a yellow filter (010 Medium Yellow from LEE filters) was placed in front of the PD when needed. According to its specifications, the PDA10A photodetector electrical bandwidth is 150 MHz. On the other hand, the LED driver was designed to have a flat response up to 100 MHz. Thus, the contribution of these components to the frequency response of the VLC link can be neglected as the maximum frequency measured in the setup is 50 MHz.

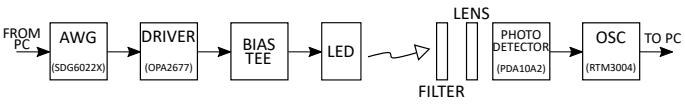

Fig. 5. Scheme of the white LED characterization setup.

Three different white LEDs were characterized:

- LED1: CXB1830-0000-000N0BV265E from Cree;
- LED2: XHP70A-01-0000-0D0BN40E1 from Cree;
- LED3: LZ4-40CW08-0065 from OSRAM.

They are shown in Fig. 6 and their main features are summarized in Table I. All three devices exhibit high luminous flux. LED1 is a COB (chip-on-board) diode type and LED2 and LED3 are composed of 4 LEDs connected in series.

TABLE I
LEDs features

Feature	LED1	LED2	LED3
Correlated Color Temperature	6500	6500	6500
Forward Voltage (V)	35	12	12.6
DC Forward Current (mA)	800	1050	700
Luminous Flux (lm)	4600	1900	800
Viewing angle (deg.)	115	120	90

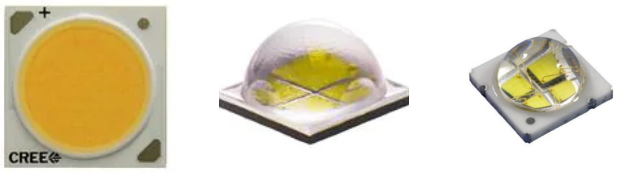

(a) (b) (c)

Fig. 6. (a) LED1; (b) LED2; (c) LED3.

A. Method to extract the model parameters

The steps required to obtain the model parameters are described below:

Step 1: $H_b(s)$ parameter extraction

1) Measure the LED frequency response with a blue filter, $|H_{b\_m}(f)|$.
2) Calculate k_b=$|H_{b\_m}(f_L)|$, where f_L is the lowest frequency to be measured.
3) Find $f_{p_{b1}}$ as $|H_{b\_m}(f_L)|_{dB}-|H_{b\_m}(f_{p_{b1}})|_{dB}$=3 dB and calculate the pole p_{b1}=$2\pi f_{p_{b1}}$.
4) Calculate $H_b(f)$ from Eq. 4 including k_b and p_{b1} and assuming p_{b2}=∞.
5) Find $f_{p_{b2}}$ as $|H_b(f_{p_{b2}})|_{dB}-|H_{b\_m}(f_{p_{b2}})|_{dB}$=3 dB and calculate the pole p_{b2}=$2\pi f_{p_{b2}}$.
6) Recalculate $H_b(f)$ from Eq. 4 including p_{b2} and check that $|H_b(f)|$ and $|H_{b\_m}(f)|$ match; if not, adjust the parameters. Note that this adjustment is necessary when p_{b1} and p_{b2} are close enough to interact with each other.

Step 2: $H_p(s)$ parameter extraction

1) Measure the LED frequency response with a yellow filter, $|H_{y\_m}(f)|$.
2) Calculate k_p=$|H_{y\_m}(f_L)|/k_b$.
3) Calculate $H_y(f)$ from Eq. 6 including k_p and assuming p_p=∞.
4) Find f_{p_p} as $|H_y(f_p)|_{dB}-|H_{y\_m}(f_{p_p})|_{dB}$=3 dB and calculate the pole p_p=$2\pi f_{p_p}$.
5) Recalculate $H_y(f)$ from Eq. 6 including p_p and check that $|H_y(f)|$ and $|H_{y\_m}(f)|$ match; if not, adjust the parameters.

Step 3: γ_b and γ_y estimations to complete $H_w(s)$

1) Measure the LED frequency response without any filter, $|H_{w\_m}(f)|$.
2) Minimize the mean squared error (MSE) according to Eq. 9 to estimate γ_b and γ_y.

$$\text{MSE} = \frac{1}{N}\sum_{f_n=f_L}^{f_H}\left(|H_w(f_n)|_{dB} - |H_{w\_m}(f_n)|_{dB}\right)^2, \quad (9)$$

where N is the number of frequency bins between f_L and f_H, and f_H is selected as the highest measured frequency not affected by noise.

3) Calculate $H_w(f)$ from Eq. 7 including γ_b and γ_y and check that $|H_w(f)|$ and $|H_{w\_m}(f)|$ match; if not, adjust the parameters.

Regarding the fine adjustment required at the end of each step, it should be noted that all parameters have a well-defined physical function (*i.e.*, a gain or a pole), so they can be easily adjusted by trial and error if both the estimated and measured frequency responses are plotted together. On the other hand, if the blue component of a white LED had a response with conjugated complex poles, the proposed model would also be suitable. In such a case, p_{b1} and p_{b2} would be complex conjugates and only Step 1.3 and Step 1.5 of the method would have to be modified to estimate those poles.

Next, an example of the application of this procedure is explained for LED1, and the results of its application are also shown for LED2 and LED3.

B. Measurements and estimations

LED1, LED2 and LED3 were biased at 400 mA, 620 mA and 650 mA, respectively, during the measurements. In order to measure the frequency response, sinusoidal signals with different frequencies were transmitted sequentially and the received power at the photodiode output was measured individually. The amplitude of the transmitted sinusoidal signals was around 200 mA and it was checked that the nonlinearities of the LEDs did not affect the measurement. Next, the method to extract the model parameters is particularized for LED1 as an example. For the sake of clarity, fine adjustment of parameters (final point of each Step) has been omitted.

Firstly, the frequency response with a blue filter, $|H_{b\_m}(f)|$, measured in Step 1.1 is shown in Fig. 7. In Step 1.2, parameter k_b is directly obtained as it is the gain at low frequency ($|H_{b\_m}(f_L)|_{dB}$ = −24.5 dB), so k_b=$10^{-24.5/20}$= $6{\cdot}10^{-2}$. The frequency of the first pole in $H_b(f)$, $f_{p_{b1}}$, is found at 2.3 MHz applying Step 1.3, and its value is p_{b1}=$1.45{\cdot}10^7$ s^{-1}. In Step 1.4, $H_b(f)$ is calculated using the estimated k_b and p_{b1} and considering that p_{b2}=∞ (as if it were a 1^{st}-order approximation). Then, the frequency of the second pole $f_{p_{b2}}$ is found at 9.4 MHz applying Step 1.5, and its value is p_{b2}=$5.91{\cdot}10^7$ s^{-1}. The estimated frequency response, $|H_b(f)|$, is shown in Fig. 7 matching the measured one, $|H_{b\_m}(f)|$.

Secondly, in Step 2.1, the LED frequency response with a yellow filter is measured ($|H_{y\_m}(f)|$ in Fig. 7). In Step 2.2, parameter k_p is indirectly obtained using the measured gain at low frequency ($|H_{y\_m}(f_L)|_{dB}$ = −3.34 dB) and k_b from Step 1: k_p=$10^{-3.34/20}/6{\cdot}10^{-2}$=11.5. $H_y(f)$ is calculated in Step 2.4 assuming p_p=∞ and used in Step 2.4 to find the pole frequency, f_{p_p}, of the phosphor coating response, $H_p(f)$, at 3.1 MHz, whose value is p_p=$1.95{\cdot}10^7$ s^{-1}. The estimated frequency response, $|H_y(f)|$, is shown in Fig. 7 matching the one measured with the yellow filter, $|H_{y\_m}(f)|$.

Finally, in Step 3.1, the LED frequency response without filters (white light) is measured ($|H_{w\_m}(f)|$ in Fig. 7). Parameters γ_b and γ_y from Eq. 7 are estimated in Step 3.2 to match the white light response. To find their values the mean squared error is minimized according to Eq. 9, where the MSE is calculated for N frequency bins between f_L = 500 kHz and f_H = 40 MHz. In the MSE calculation both responses are used in logarithmic format to enable a better fit at higher frequencies. As they have greater magnitude at low frequencies, if the MSE is calculated with frequency responses in linear format, the obtained result has a poorer match at higher frequencies. As only two parameters γ_b and γ_y must be found, an exhaustive search was employed. The obtained γ_b and γ_y are shown in Table II together with the rest of the parameters and Fig. 7 shows how the white LED1 estimated response, $|H_w(f)|$, matches the measured one, $|H_{w\_m}(f)|$.

TABLE II
ESTIMATED LEDS PARAMETERS

Parameters	LED1	LED2	LED3
k_b	$6{\cdot}10^{-2}$	$5.9{\cdot}10^{-2}$	$6.0{\cdot}10^{-2}$
$p_{b1}(s^{-1})$	$1.45{\cdot}10^7$	$1.26{\cdot}10^7$	$2.01{\cdot}10^7$
$p_{b2}(s^{-1})$	$5.91{\cdot}10^7$	$7.54{\cdot}10^7$	$12.56{\cdot}10^7$
k_p	11.5	8.5	8.2
$p_p(s^{-1})$	$1.95{\cdot}10^7$	$2.07{\cdot}10^7$	$2.20{\cdot}10^7$
γ_b	3.4	3.25	3
γ_y	1.09	1.04	1.05

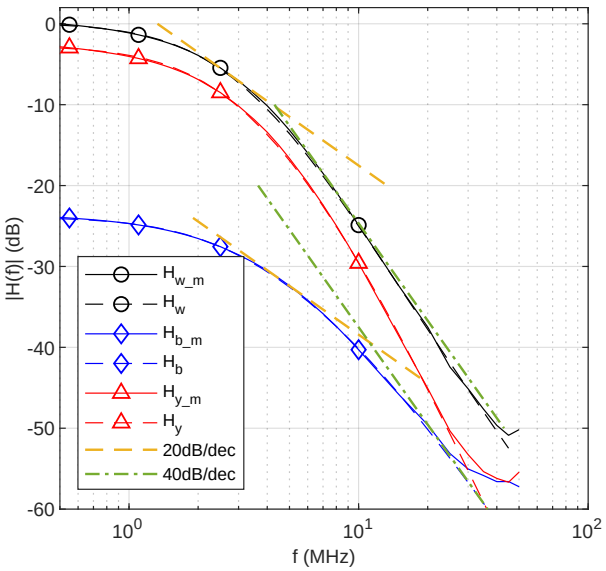

Fig. 7. Measured (solid line) and estimated (dashed line) frequency response of LED1.

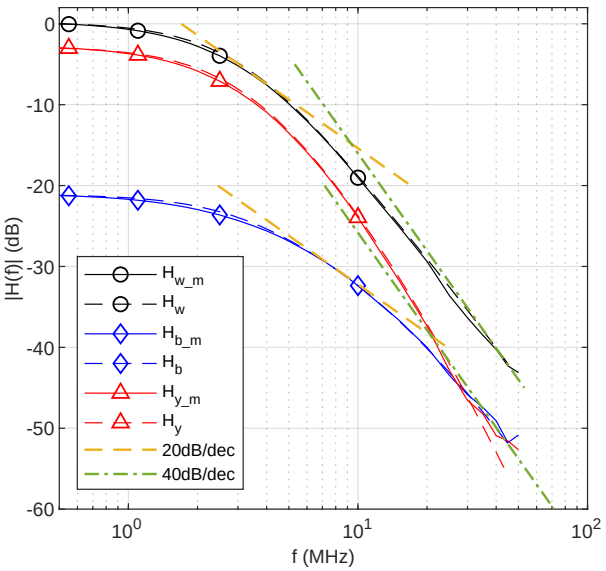

Fig. 9. Measured (solid line) and estimated (dashed line) frequency response of LED3.

The same procedure was followed for LED2 and LED3 and their parameters are also indicated in Table II and their respective frequency responses are shown in Fig. 8 and 9. Observing Figs. 7 to 9, it can be stated that a very good match between the proposed model and the measurements for all three white LEDs is obtained. The slight disagreement at high frequencies is due to the high attenuation (above 40 dB) suffered by the detected signal at those frequencies, which rendered noisier measured values.

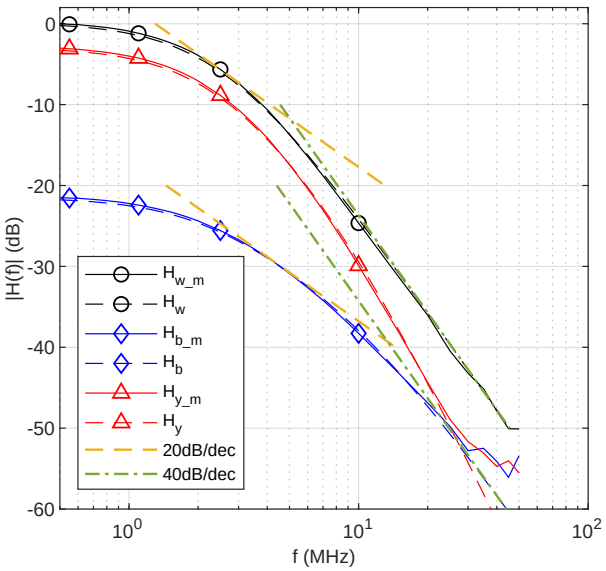

Fig. 8. Measured (solid line) and estimated (dashed line) frequency response of LED2.

C. Analysis

Table III shows the frequencies of the poles due to the blue LED and the phosphor coating, obtained from Table II as f_{pi}=$p_i/2\pi$. As can be seen, f_{pb1} and f_{pb2} are in the measurement frequency range, so the 2^{nd}-order effect appears in Figs. 7 to 9, where the slopes of $|H_{b\_m}(f)|$ are higher than −20 dB/dec (which is the slope of a 1^{st}-order system). Regarding the phosphor coating, its pole (f_{p_p}) is around 3.3 MHz for all three LEDs, which is consistent with the values measured by other authors [7].

From the results in Table II, the ratio between blue and yellow light components can be obtained as $\gamma_b/(\gamma_y \cdot k_p)$, in terms of detected optical power or photodetected current. The results are 21%/79%, 27%/73% and 26%/74% for LED1, LED2 and LED3, respectively. These proportions correspond to cool white LEDs as expected from their color temperature shown in Table I. As γ_b and γ_y are obtained in Step 3 of the proposed method, when the white LED response is measured without filter, the transmissivity of the blue and yellow filters does not affect the obtained ratios. However, the actual ratio of blue and yellow optical power generated in the LED could be slightly different from these values as long as the responsivity of the photodetector is not constant at the corresponding wavelength bands.

It is important to remark that the most important specification in order to select the blue and yellow filters is the out-of-band rejection of each filter, so that the frequency response of the blue or yellow components are only measured in terms of blue or yellow photons, respectively.

As explained in Section III-C, the white LED transfer function (Eq. 8) includes a zero that depends on the phosphor pole and the proportion in which the yellow and blue lights are combined. Its frequency is also included in Table III.

It can be seen that the three LEDs follow a similar pat-

TABLE III
ESTIMATED FREQUENCIES OF POLES AND ZERO GIVEN IN MHZ

pole/zero	LED1	LED2	LED3
$f_{p_{b1}}$	2.3	2	3.2
$f_{p_{b2}}$	9.4	12	20
f_{p_p}	3.1	3.3	3.5
f_{z_p}	14.5	12.2	13.5

tern. Their frequency response is dominated by the low-frequency poles from the blue LED ($f_{p_{b1}}$) and the phosphor coating (f_{p_p}), which are quite close to each other, between 2 and 3.5 MHz. Both poles conform the 2^{nd}-order slope of −40 dB/dec of the white LED frequency response. The slope of the blue LED frequency response changes gradually from −20 dB/dec to −40 dB/dec beyond its second pole. In the same way, the frequency response of the yellow component also starts to change its slope to −60 dB/dec (the slope of a 3^{rd}-order system) from this point. However, in the white LED, both the second pole of the blue LED ($f_{p_{b2}}$) and the zero (f_{z_p}) appear at similar frequencies. As they are very close to each other ($f_{p_{b2}}$ = 9.4 MHz and f_{z_p} = 14.5 MHz for LED1), their slopes tend to cancel, and they hardly influence the response of the white LED. Therefore, the yellow component is attenuated faster (−60 dB/dec) than the blue component (−40 dB/dec) at high frequency, in such a way that the slope of the white LED frequency response follows the −40 dB/dec slope of the blue light even though the yellow component is dominant at low frequencies.

This analysis is shown graphically in Fig. 10. This figure shows the measured frequency response, the estimated response from (Eq. 8) and the Bode asymptotes using the frequencies shown in Table III. In general, the position of the poles and the zero influences the deviation between the Bode plot and the frequency response. In this case, $f_{p_{b1}}$ and f_{p_p} are quite close, so this deviation is about 6 dB. Besides, the short distance between the pole at ($f_{p_{b2}}$) and the zero at (f_{z_p}) makes unnoticeable the −60 dB/dec trend between both frequencies.

V. CONCLUSION

Although the response of ideal LEDs can be modeled as a 1^{st}-order system, commercial high-luminous flux white LEDs connected in a realistic lighting environment exhibit a higher-order frequency response due to the parasitic effects introduced by the components required for their mounting. We have proposed a new model for these white LEDs that enhances their frequency characterization, and enables a more reliable simulation of VLC links. In addition, a systematic method to estimate the model parameters is presented, based on the measurement of the blue, yellow and white components of the emitted light, obtained by using two optical filters (blue and yellow). The model was used to characterize three different white LEDs, matching measured and estimated frequency responses up to around 45 MHz.

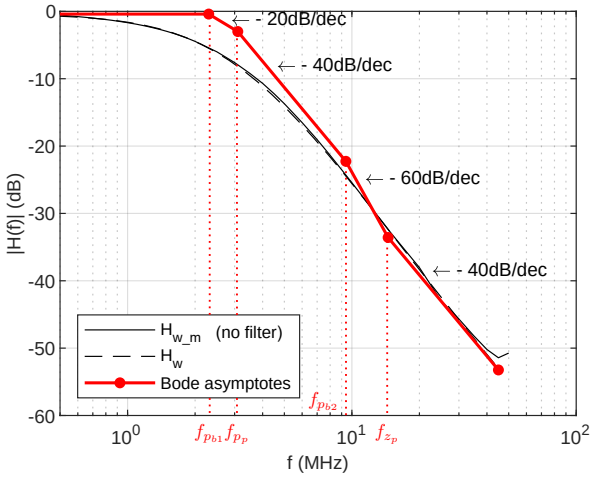

Fig. 10. Measured (solid line) and estimated (dashed line) frequency response of LED1 and its Bode asymptotes.

REFERENCES

[1] A. Tsiatmas, C. P. Baggen, F. M. Willems, J.-P. M. Linnartz, and J. W. Bergmans, "An illumination perspective on visible light communications," *IEEE Communications Magazine*, vol. 52, no. 7, pp. 64–71, 2014.

[2] H. Haas, L. Yin, Y. Wang, and C. Chen, "What is LiFi?" *Journal of Lightwave Technology*, vol. 34, no. 6, pp. 1533–1544, 2016.

[3] T. P. Lee, "Effect of junction capacitance on the rise time of LED's and on the turn-on delay of injection lasers," *The Bell System Technical Journal*, vol. 54, no. 1, pp. 53–68, 1975.

[4] H. Le Minh, D. O'Brien, G. Faulkner, L. Zeng, K. Lee, D. Jung, Y. Oh, and E. T. Won, "100-mb/s nrz visible light communications using a postequalized white led," *IEEE Photonics Technology Letters*, vol. 21, no. 15, pp. 1063–1065, 2009.

[5] S. Mardanikorani, X. Deng, and J.-P. M. G. Linnartz, "Sub-carrier loading strategies for DCO-OFDM LED communication," *IEEE Transactions on Communications*, vol. 68, no. 2, pp. 1101–1117, 2020.

[6] C. Chen, D. A. Basnayaka, and H. Haas, "Downlink performance of optical attocell networks," *Journal of Lightwave Technology*, vol. 34, no. 1, pp. 137–156, 2016.

[7] D. Xue, C. Ruan, Y. Zhang, H. Chen, X. Chen, C. Wu, C. Zheng, H. Chen, and W. W. Yu, "Enhanced bandwidth of white light communication using nanomaterial phosphors," *Nanotechnology*, vol. 29, no. 45, 2018.

[8] G. Stepniak, M. Schüppert, and C.-A. Bunge, "Advanced modulation formats in phosphorous led VLC links and the impact of blue filtering," *Journal of Lightwave Technology*, vol. 33, no. 21, pp. 4413–4423, 2015.

[9] X. Li, Z. Ghassemlooy, S. Zvanovec, M. Zhang, and A. Burton, "Equivalent circuit model of high power leds for VLC systems," in *2019 2nd West Asian Colloquium on Optical Wireless Communications (WACOWC)*, 2019, pp. 90–95.

[10] X. Li, Z. Ghassemlooy, S. Zvanovec, and L. N. Alves, "An equivalent circuit model of a commercial LED with an ESD protection component for VLC," *IEEE Photonics Technology Letters*, vol. 33, no. 15, pp. 777–779, 2021.

[11] P.-C. Song, Z.-Y. Wu, X.-D. An, and J. Wang, "Energy efficiency analysis of light-emitting diodes with high modulation bandwidth," *IEEE Electron Device Letters*, vol. 42, no. 7, pp. 1025–1028, 2021.

[12] H. Le Minh, D. O'Brien, G. Faulkner, L. Zeng, K. Lee, D. Jung, and Y. Oh, "High-speed visible light communications using multiple-resonant equalization," *IEEE Photonics Technology Letters*, vol. 20, no. 14, pp. 1243–1245, 2008.